*Electronic Journal of Differential Equations*, Vol. 2025 (2025), No. 38, pp. 1–19.
ISSN: 1072-6691. URL: https://ejde.math.txstate.edu, https://ejde.math.unt.edu
DOI: 10.58997/ejde.2025.38

# TRAVELING WAVES OF A DIFFUSIVE MODIFIED LESLIE-GOWER MODEL WITH CHEMOTAXIS

SHUNA WANG, JIANG LIU, JUN FANG, XIAOJIE LIN

Abstract. In this article, we study a diffusive modified Leslie-Gower model with chemotaxis and large wave speed. By applying traveling wave transformation and changing the time scale, this modified Leslie-Gower model can be transformed into a singularly perturbed system. We establish the existence of heteroclinic orbits connecting different equilibria for the system without perturbation by constructing invariant regions and using the Poincaré-Bendixson theorem. Then the existence of traveling wave solutions for the diffusive modified Leslie-Gower system is demonstrated via the geometric singular perturbation theory and Fredholm theory.

## 1. Introduction

In ecosystems there exist a large number of predation relationships among species. Numerous scholars have conducted a series of investigations into interactions between predators and prey [9, 11, 19, 30], which play an important role in revealing the dynamic evolution of populations. To describe that the population density of predator is restricted by preys, Leslie and Gower [15, 16] improved the classical Lotka-Volterra model [20, 28] and proposed the Leslie-Gower model

$$
\begin{aligned}
\frac{du}{dt} &= u(\alpha_1 - \beta u - \theta_1 v),\\
\frac{dv}{dt} &= v(\alpha_2 - \frac{\theta_2 v}{u}),
\end{aligned}
\tag{1.1}
$$

where $u$ and $v$ represent the density of the prey and predator, respectively. The increase of the predator population follows the logistic growth model. The carrying capacity of environment is positively correlated with the number of prey population.

Based on the Leslie-Gower model (1.1), many modified versions have been considered. As mentioned in [1], the predator can seek alternative food for survival instinct if its preferred food is extremely scarce. Due to the scarcity of preferred food, the growth rate of predator can decline. To model this ecological phenomenon, authors added a constant $k$ to the system (1.1), and yielded

$$
\begin{aligned}
\frac{du}{dt} &= u(\alpha_1 - \beta u - \theta_1 v),\\
\frac{dv}{dt} &= v(\alpha_2 - \frac{\theta_2 v}{u+k}),
\end{aligned}
\tag{1.2}
$$

where $k$ represents the maximum decline rate to indicate the environmental protection.

Models (1.1) and (1.2) are both ordinary differential equations, which are constructed based on the assumption that the spatial distribution of populations is uniform. However, the uneven distribution of resources leads to an unbalanced spatial distribution of organisms in nature. In order to survive, the population may migrate and diffuse from high density areas to low density areas.

2020 *Mathematics Subject Classification.* 35K57, 92D25, 35C07, 34D15.
*Key words and phrases.* Modified Leslie-Gower model; chemotaxis; traveling waves;
geometric singular perturbation.

Submitted February 21, 2025. Published April 10, 2025.

Mathematically, this phenomenon can be described by the self-diffusion of species. Therefore, many researchers focused on the following reaction-diffusion system with Leslie-Gower term

$$\begin{aligned} \frac{\partial u}{\partial t} &= d_1 \Delta u + u(\alpha_1 - \beta u - \theta_1 v), \\ \frac{\partial v}{\partial t} &= d_2 \Delta v + v(\alpha_2 - \frac{\theta_2 v}{u}). \end{aligned} \tag{1.3}$$

Several investigations have been carried out with respect to model (1.3). Du and Hsu [4] proved the existence of postively steady-state solutions with prescribed spatial patterns. Moreover, they compared with the classical Lotka-Volterra model, some crucial differences in the dynamic behavior were observed. Hamizah M. Safuan et al. [26] found the existence of traveling waves and derived the minimum wave speed. Furthermore, they also carried out the stability of traveling waves. With the use of the Lyapunov function and the transformation technique, Zhou and Wei [33] obtained a new global stability result of the positive equilibrium and generalized results to the more general reaction-diffusion system.

In addition to the self-diffusion of predator and prey, the diffusion of predator may be influenced by prey. This influence gives rise to chemotactic movement, making the predator population migrate towards areas of high prey density. In 1987, based on the data of prey gliding in ladybugs, Kareiva and Odell [13] firstly proposed a predator-prey system with prey-taxis to explain the predation between ladybugs and aphids. In the ecological system, chemotaxis plays an significant role in maintaining ecological balance and biodiversity, such as regulating prey species (pest) to prevent outbreaks. Furthermore, models incorporating chemotaxis may produce different spatial patterns and bring new dynamical behaviors. Recently, Li [17] studied a two-species system with chemotaxis

$$\begin{aligned} \frac{\partial u}{\partial t} &= \Delta u + u(\alpha_1 - \beta u - \theta_1 v), \\ \frac{\partial v}{\partial t} &= \Delta v - \chi \nabla \cdot (v \nabla u) + \vartheta uv - \varrho v, \end{aligned} \tag{1.4}$$

where the chemotaxis term $\chi \nabla \cdot (v \nabla u)$ expresses the tendency of the predator to move upward or downward along the gradient direction of prey, and $\chi$ denotes the prey-taxis coefficient. When $\chi > 0$ ($\chi < 0$), the chemotaxis is characterized as attractive (repulsive). From a biological perspective, $\chi > 0$ implies that predator tends to diffuse towards areas where the density of prey is higher to enhance capture rate; Conversely, $\chi < 0$ represents the predator tends to diffuse towards areas where the density of prey is lower to avoid prey group defense. That is, the spatiotemporal dynamics of predators is influenced by the prey density. Under Neumann boundary conditions, Li proved that system (1.4) admits a unique global bounded classical solution. Currently, various biological models with chemotaxis have been proposed and extensively studied [6, 18, 22]. Zhao and Hu in [31] investigated the classical solutions of a prey-taxis model with Sigmoid function response under homogeneous Neumann boundary conditions. Moreover, they demonstrated that the prey-taxis sensitivity coefficient destabilizes the stability of the homogeneous steady state when the prey defend. Qiu and Guo [24] focused on a Leslie-Gower model with chemotaxis. Based on the asymptotic analysis and bifurcation theory, they obtained the local and global bifurcation of nonconstant steady-states by taking the chemotaxis coefficient as a bifurcation parameter.

Inspired by the above mentioned papers, we investigate the diffusion model with chemotaxis

$$\begin{aligned} \frac{\partial u}{\partial t} &= d_1 \Delta u + a_1 u(1 - b_1 u - r_1 v), \\ \frac{\partial v}{\partial t} &= d_2 \Delta v + \chi \nabla \cdot (v \nabla u) + a_2 v(1 - \frac{r_2 v}{u + k}), \end{aligned} \tag{1.5}$$

where $u$ and $v$ respectively represent the density of the prey and predator at spatial position $x$ and time $t$. $d_1$ and $d_2$ are diffusion coefficients of populations. $\nabla \cdot (v \nabla u)$ accounts for the chemotaxis phenomenon. $\chi > 0$ stands for the sensitivity of chemotaxis. $a_1$ and $a_2$ response the intrinsic growth rate of prey and predator. $b_1$ reflects the intensity of competition among members of prey species. $r_1$ and $r_2$ are the maximum values of the average decrease rate for organisms. $k$ indicates the environmental protection. All the parameters mentioned above are positive.

For biological population systems, traveling waves can describe the behaviors of species, such as propagation, migration, and invasion. Therefore, studying the traveling waves of population systems has great significance. In recent years, the qualitative properties of the traveling waves of the Leslie-Gower model have also been widely studied [2, 8, 25, 27]. For example, Tian and Zhang [27] explored the traveling waves for a modified Leslie-Gower model with continuous diffusion or discrete diffusion based on the squeeze method and a Lyapunov function. Guo and Cheng [8] considered a prey-predator system of Leslie-Gower type under shifting environment, and the existence of traveling waves was proved by utilizing the method of constructing the suitable upper and lower solution with a monotone iteration technique.

On the other hand, the interactions of populations occur on different time scales in nature. The dynamical behaviors observed in these systems also reflect these multi-scale characteristics [3, 10]. The main theoretical basis for studying such problems is the geometric singular perturbation theory [7, 12]. In recent years, the geometric singular perturbation theory has also been widely applied to many other equations [5, 21, 29, 32].

In this article, we focus on the existence of traveling waves for the modified Leslie-Gower model with chemotaxis (1.5) and large wave speed. The highlights of our paper mainly lie in the following aspects.

• Several Leslie-Gower models investigated in previous works can be considered as special instances of our model. This includes the models presented in references [26, 23].

• We transform the modified Leslie-Gower model with chemotaxis (1.5) into a fast-slow system. And the existence of traveling waves that connect different equilibrium points can be obtained by applying the geometric singular perturbation theory.

• We obtain two types of traveling waves when system (1.5) has no co-existence equilibrium and three types of traveling waves when system (1.5) admits the co-existence equilibrium. Then we generalize the results obtained in [18], which proved the existence of traveling waves between the co-existence equilibrium and $(0, 0)$.

The rest of this article is structured as follows. In Section 2, we provide the geometric singular perturbation theory and present some preliminaries on system (1.5). In Section 3, the existence of heteroclinic solutions for the slow subsystem (2.12) is proved, based on the phase plane analysis along with Poincaré-Bendixson theorem. In Section 4, the existence of the traveling waves for system (1.5) is established via the application of geometric singular perturbation theory and Fredholm theory. In Section 5, we present a main summary of our findings.

## 2. Preliminaries

In this section, we outline the geometric singular perturbation theory. Moreover, we investigate the existence and stability of boundary equilibria and the co-existence equilibrium.

### 2.1. Geometric singular perturbation theory.

Firstly, we introduce the definitions and conclusions related to geometric singular perturbation [12, 14]. Consider the differential equations

$$\begin{aligned} x' &= f(x, y, \varepsilon), \\ y' &= \varepsilon g(x, y, \varepsilon), \end{aligned} \tag{2.1}$$

where $' = \frac{d}{dt}$ denotes the differentiation with respect to the fast time scale $t$. Fast variable $x \in \mathbb{R}^p$, slow variable $y \in \mathbb{R}^q$ with $p, q \geq 1$, $f : \mathbb{R}^p \times \mathbb{R}^q \times \mathbf{R} \to \mathbb{R}^p$, $g : \mathbb{R}^p \times \mathbb{R}^q \times \mathbf{R} \to \mathbb{R}^q$. The functions $f$ and $g$ are sufficiently smooth. And the positive parameter $\varepsilon$ is sufficiently small, which can be regarded as separation of time scales. Set $t = \frac{\tau}{\varepsilon}$, (2.1) has the equivalent form

$$\begin{aligned} \varepsilon \dot{x} &= f(x, y, \varepsilon), \\ \dot{y} &= g(x, y, \varepsilon), \end{aligned} \tag{2.2}$$

where $\cdot = \frac{d}{d\tau}$ denotes the differentiation with respect to the slow time scale $\tau$. Based on the relationship between $t$ and $\tau$, system (2.1) and system (2.2) are referred to as the fast system and slow system.

Setting $\varepsilon = 0$ in (2.1) and (2.2), one has the fast subsystem (layer system)

$$\begin{aligned} x' &= f(x, y, 0), \\ y' &= 0, \end{aligned} \tag{2.3}$$

and the slow subsystem (reduced system)

$$\begin{aligned} 0 &= f(x, y, 0), \\ \dot{y} &= g(x, y, 0). \end{aligned} \tag{2.4}$$

**Definition 2.1.** The set defined by the algebraic equations in the slow subsystem (2.4)

$$M = \{(x, y) \in \mathbb{R}^p \times \mathbb{R}^q : f(x, y, 0) = 0\}$$

is called the critical set, which is also the set of equilibria for the fast subsystem (2.3). If $M$ is a submanifold of $\mathbb{R}^p \times \mathbb{R}^q$, then $M$ is referred to as a critical manifold.

**Definition 2.2.** The critical manifold $M$ is normally hyperbolic if the linearization of (2.3) at all point on $M$ has exactly $p$ eigenvalues off the imaginary axis.

**Lemma 2.3** ([12, 14])**.** *Consider the system* (2.1)*, if submanifold $M_0$ of critical manifold $M$ is compact and normally hyperbolic, then for $0 < r < +\infty$ and $0 < \varepsilon \ll 1$, the following conclusions hold,*

(i) *there exists a slow manifold $M_\varepsilon$ that lies within $\mathcal{O}(\varepsilon)$ of $M_0$ is diffeomorphic to $M_0$, and $M_\varepsilon$ is locally invariant under the flow of* (2.1)*. This means that the flow of system* (2.1) *only can enter or leave through the boundary of $M_\varepsilon$;*

(ii) *there exist $C^r$-smooth unstable manifolds $W^u_{\rm loc}(M_\varepsilon)$ and stable manifolds $W^s_{\rm loc}(M_\varepsilon)$, which are $\mathcal{O}(\varepsilon)$ close to and diffeomorphic to $W^u_{\rm loc}(M_0)$ and $W^s_{\rm loc}(M_0)$, respectively. In addition, $W^u_{\rm loc}(M_\varepsilon)$ and $W^s_{\rm loc}(M_\varepsilon)$ are locally invariant with respect to the flow of system* (2.1)*.*

**Definition 2.4.** A traveling wave solution of system (1.5) can be expressed as

$$z = x - ct, \quad (u, v)(x, t) = (U, V)(z), \tag{2.5}$$

where $c > 0$ represents the wave speed.

Applying the traveling wave transformation (2.5) to system (1.5), we obtain the wave profile system

$$\begin{aligned} -cU_z &= d_1 U_{zz} + a_1 U(1 - b_1 U - r_1 V), \\ -cV_z &= d_2 V_{zz} + \chi(U_z V_z + U_{zz} V) + a_2 V(1 - \frac{r_2 V}{U + k}), \end{aligned} \tag{2.6}$$

where $U_z = \frac{dU}{dz}$ and $U_{zz} = \frac{d^2U}{dz^2}$.

Setting $\xi = -\frac{z}{c}$, system (2.6) is transformed into

$$\begin{aligned} \varepsilon \ddot{U} &= \dot{U} - a_1 U(1 - b_1 U - r_1 V), \\ \varepsilon \ddot{V} &= \frac{1}{\rho}\dot{V} - \varepsilon\gamma(\dot{U}\dot{V} + \ddot{U}V) - \frac{a_2}{\rho} V(1 - \frac{r_2 V}{U + k}), \end{aligned} \tag{2.7}$$

where $\dot{} = \frac{d}{d\xi}$, $\rho = \frac{d_2}{d_1}$, $\gamma = \frac{\chi}{d_1 \rho}$ and $\varepsilon = \frac{d_1}{c^2}$ satisfying $0 < \varepsilon \ll 1$. System (2.7) is equivalent to the slow syetem

$$\begin{aligned} \dot{U} &= U_1, \\ \dot{V} &= V_1, \\ \varepsilon \dot{U}_1 &= U_1 - a_1 U(1 - b_1 U - r_1 V), \\ \varepsilon \dot{V}_1 &= -\varepsilon\gamma U_1 V_1 - \gamma V[U_1 - a_1 U(1 - b_1 U - r_1 V)] \\ &\quad + \frac{1}{\rho} V_1 - \frac{a_2}{\rho} V(1 - \frac{r_2 V}{U + k}), \end{aligned} \tag{2.8}$$

where $\xi$ indicates the slow time scale. Setting $\zeta = \frac{\xi}{\varepsilon}$ in system (2.8) results in the fast system

$$
\begin{aligned}
U' &= \varepsilon U_1,\\
V' &= \varepsilon V_1,\\
U_1{}' &= U_1 - a_1 U(1 - b_1 U - r_1 V),\\
V_1{}' &= -\varepsilon\gamma U_1 V_1 - \gamma V[U_1 - a_1 U(1 - b_1 U - r_1 V)] + \frac{1}{\rho}V_1 - \frac{a_2}{\rho}V(1 - \frac{r_2 V}{U+k}),
\end{aligned}
\tag{2.9}
$$

where $' = \frac{d}{d\zeta}$, and $\zeta$ indicates the fast time scale. Setting $\varepsilon = 0$ in slow system (2.8) and fast system (2.9), we respectively obtain the slow subsystem

$$
\begin{aligned}
\dot U &= U_1,\\
\dot V &= V_1,\\
0 &= U_1 - a_1 U(1 - b_1 U - r_1 V),\\
0 &= \frac{1}{\rho}V_1 - \frac{a_2}{\rho}V(1 - \frac{r_2 V}{U+k}),
\end{aligned}
\tag{2.10}
$$

and the fast subsystem

$$
\begin{aligned}
U' &= 0,\\
V' &= 0,\\
U_1{}' &= U_1 - a_1 U(1 - b_1 U - r_1 V),\\
V_1{}' &= -\gamma V[U_1 - a_1 U(1 - b_1 U - r_1 V)] + \frac{1}{\rho}V_1 - \frac{a_2}{\rho}V(1 - \frac{r_2 V}{U+k}).
\end{aligned}
\tag{2.11}
$$

Based on Definition 2.1, the critical manifold of fast system (2.9) is

$$
M_0 = \big\{(U, U_1, V, V_1) : U_1 = a_1 U(1 - b_1 U - r_1 V), V_1 = a_2 V(1 - \frac{r_2 V}{U+k})\big\},
$$

which is two-dimensional and consists of equilibria of the fast subsystem (2.11).

The Jacobian matrix of system (2.11) at any point of $M_0$ reads

$$
\begin{pmatrix}
0 & 0 & 0 & 0\\
0 & 0 & 0 & 0\\
-a_1(1 - 2b_1 U - r_1 V) & a_1 r_1 U & 1 & 0\\
a_1\gamma V(1 - 2b_1 U - r_1 V) - \frac{a_2 r_2 V^2}{\rho(U+k)^2} & W(U, V, U_1) & -\gamma V & \frac{1}{\rho}
\end{pmatrix},
$$

where $W(U, V, U_1) = -\gamma U_1 + a_1\gamma U(1 - b_1 U - 2r_1 V) + \frac{a_2}{\rho}(\frac{2r_2 V}{U+k} - 1)$.

After computations, we obtain that the matrix has two positive eigenvalues 1, $\frac{1}{\rho}$, and two zero eigenvalues. Therefore, the dimension of the fast variables is equal to the number of eigenvalues off the imaginary axis. By Definition 2.2, we deduce that the critical manifold $M_0$ is normally hyperbolic. According to Lemma 2.3, for $0 < \varepsilon \ll 1$, there exists a perturbed locally invariant manifold $M_\varepsilon$ which is $\mathcal{O}(\varepsilon)$-close to $M_0$.

2.2. **Equilibria of the slow subsystem** (2.12)**.** The dynamics behavior restricted on $M_0$ is determined by the slow subsystem

$$
\begin{aligned}
\dot U &= a_1 U(1 - b_1 U - r_1 V),\\
\dot V &= a_2 V(1 - \frac{r_2 V}{U+k}).
\end{aligned}
\tag{2.12}
$$

The existence and topological properties of boundary equilibria for the slow subsystem (2.12) can be characterized by the following lemma.

**Lemma 2.5.** *The slow subsystem* (2.12) *admits three boundary equilibria* $E_0(0,0)$*,* $E_1(\frac{1}{b_1}, 0)$ *and* $E_2(0, \frac{k}{r_2})$*. Among them,*

(i) $E_0$ *is always an unstable node;*

(ii) *$E_1$ is always a saddle;*
(iii) *$E_2$ is a stable node for $0 < r_2 < r_1 k$, $E_2$ is a saddle for $r_2 > r_1 k$, and $E_2$ is a saddle-node for $r_2 = r_1 k$.*

*Proof.* It is evident that the slow subsystem (2.12) admits three boundary equilibria $E_0(0,0)$, $E_1(\frac{1}{b_1},0)$ and $E_2(0,\frac{k}{r_2})$.

(i) The linearized matrix of the slow subsystem (2.12) at $E_0(0,0)$ is

$$J(E_0) = \begin{pmatrix} a_1 & 0 \\ 0 & a_2 \end{pmatrix},$$

which has two positive real eigenvalues $a_1$ and $a_2$, thus the equilibrium $E_0$ is an unstable node.

(ii) The linearized matrix of the slow subsystem (2.12) restricted to $E_1(\frac{1}{b_1},0)$ is

$$J(E_1) = \begin{pmatrix} -a_1 & -\frac{a_1 r_1}{b_1} \\ 0 & a_2 \end{pmatrix},$$

which has one negative eigenvalue $-a_1$ and one positive eigenvalue $a_2$, thus the equilibrium $E_1$ is a saddle.

(iii) The Jacobian matrix of the slow subsystem (2.12) at $E_2(0,\frac{k}{r_2})$ is

$$J(E_2) = \begin{pmatrix} a_1(1-\frac{r_1 k}{r_2}) & 0 \\ \frac{a_2}{r_2} & -a_2 \end{pmatrix}.$$

If $0 < r_2 < r_1 k$, then $1 - \frac{r_1 k}{r_2} < 0$. It follows that the matrix $J(E_2)$ has two negative real eigenvalues $a_1(1-\frac{r_1 k}{r_2})$ and $-a_2$. Thus the equilibrium $E_2$ is a stable node.

If $r_2 > r_1 k$, then $1 - \frac{r_1 k}{r_2} > 0$. One obtains that the matrix $J(E_2)$ has one positive eigenvalue $a_1(1-\frac{r_1 k}{r_2})$ and one negative eigenvalue $-a_2$, that is the equilibrium $E_2$ is a saddle.

If $r_2 = r_1 k$, then $1 - \frac{r_1 k}{r_2} = 0$. And the Jacobian matrix $J(E_2)$ has one negative real eigenvalue $-a_2$ and one zero eigenvalue, which indicates that $E_2$ is a high-order equilibrium.

To conduct a detailed analysis regarding the type of this high-order equilibrium $E_2$, we apply the linear translation $x = U$, $y = V - \frac{k}{r_2}$, which moves the equilibrium $E_2(0,\frac{k}{r_2})$ to the origin $(0,0)$. Then by rescaling time via $\xi = r_2(x+k)\tau$, the slow subsystem (2.12) becomes

$$\begin{aligned} \frac{dx}{d\tau} &= -a_1 r_2 x(x+k)(b_1 x + r_1 y), \\ \frac{dy}{d\tau} &= a_2(r_2 y + k)(x - r_2 y). \end{aligned} \tag{2.13}$$

Let $X = \frac{1}{r_2}x$ and $Y = -\frac{1}{r_2}x + y$, the system (2.13) can be rewritten as

$$\begin{aligned} \frac{dX}{d\tau} &= -a_1 r_2 k(b_1 r_2 + r_1)X^2 - a_1 r_1 r_2 kXY - a_1 {r_2}^2(b_1 r_2 + r_1)X^3 - a_1 r_1 {r_2}^2 X^2 Y, \\ \frac{dY}{d\tau} &= -a_2 r_2 kY - a_2 {r_2}^2 Y^2 + a_2 r_2 k(b_1 r_2 + r_1)X^2 + a_2 {r_2}^2 k(b_1 r_2 + r_1)X^3 \\ &\quad + a_2 r_1 {r_2}^2 X^2 Y. \end{aligned} \tag{2.14}$$

Using $d\eta = -a_2 r_2 k d\tau$ in the system (2.14) yields

$$\begin{aligned} \frac{dX}{d\eta} &= \frac{a_1(b_1 r_2 + r_1)}{a_2}X^2 + \frac{a_1 r_1}{a_2}XY + \frac{a_1 r_2(b_1 r_2 + r_1)}{a_2 k}X^3 + \frac{a_1 r_1 r_2}{a_2 k}X^2 Y, \\ \frac{dY}{d\eta} &= Y + \frac{r_2}{k}Y^2 - (b_1 r_2 + r_1)X^2 - \frac{r_2(b_1 r_2 + r_1)}{k}X^3 - \frac{r_1 r_2}{k}X^2 Y. \end{aligned} \tag{2.15}$$

Since the coefficient of $X^2$ is $\frac{a_1(b_1 r_2 + r_1)}{a_2} > 0$, $E_2$ is a saddle-node. Moreover, the parabolic sector is in the right halfplane and two hyperbolic sectors are in the left halfplane. In order to study the dynamics near $(0,0)$, we introduce the polar coordinates $X = Rcos\theta$ and $Y = Rsin\theta$. Then the system (2.15) can be given by

$$\begin{aligned}\frac{dR}{d\eta} &= -a_2r_2kRsin^2\theta - a_1r_2k(b_1r_2+r_1)R^2cos^3\theta - a_2{r_2}^2R^2\sin^3\theta\\ &\quad + [a_2r_2k(b_1r_2+r_1) - a_1r_1r_2k]R^2cos^2\theta\sin\theta + \mathcal{O}(R^3),\\ \frac{d\theta}{d\eta} &= -a_2r_2ksin\theta\cos\theta + \mathcal{O}(R).\end{aligned} \tag{2.16}$$

The polar coordinate transformation replaces dynamical behaviors near $(0,0)$ with the unit circumference $\mathbb{S}^1$. It is obvious that there are four singularities $(0,\theta_i)$ on invariant set $\{0\}\times\mathbb{S}^1$, where $\theta_i = 0, \frac{\pi}{2}, \pi, \frac{3\pi}{2}$, $i = 1,2,3,4$. For $0 < R \ll 1$, we can obtain that $\frac{dR}{d\eta} < 0$ holds along $\theta = \theta_1, \theta_2, \theta_4$, and $\frac{dR}{d\eta} > 0$ holds along $\theta = \theta_3$. In conclusion, the trajectory distribution nearby the unit circumference is illustrated in Figure 1 (a). Moreover, by reducing the unit circumference to $(0,0)$, we can get the distribution of trajectories near the origin $(0,0)$ of the $XOY$ plane, which is shown in Figure 1 (b). Therefore, any trajectory originating from $(X_0, Y_0)$ near $(0,0)$ $(X_0 \geq 0)$ will tend to the origin $(0,0)$. It follows that the equilibrium $E_2(0, \frac{k}{r_2})$ of the slow subsystem (2.12) is a attractive saddle-node.

The proof is complete. Figure 1 (c) illustrates the dynamics of the system (2.12) around $E_2$ when $a_1 = a_2 = 2$, $b_1 = r_1 = 1$, $r_2 = 5$ and $k = 5$. □

Now we show the existence and linear stability of the co-existence equilibrium.

**Lemma 2.6.** (i) *If $r_2 \leq r_1k$, the slow subsystem* (2.12) *has no co-existence equilibrium.*
(ii) *If $r_2 > r_1k$, the slow subsystem* (2.12) *has one co-existence equilibrium $E_*(\frac{r_2-r_1k}{r_1+b_1r_2}, \frac{1+b_1k}{r_1+b_1r_2})$, which is stable.*

*Proof.* The co-existence equilibrium $E_*(U_*, V_*)$ is a point that the non-trivial prey and predator isoclines intersect. It must satisfy

$$\begin{aligned}V &= -\frac{b_1}{r_1}U + \frac{1}{r_1},\\ V &= \frac{1}{r_2}U + \frac{k}{r_2}.\end{aligned}$$

By direct calculations, we can obtain that $U_* = \frac{r_2-r_1k}{r_1+b_1r_2}$ and $V_* = \frac{1+b_1k}{r_1+b_1r_2}$. Since the co-existence equilibrium $E_*(U_*, V_*)$ lies in the first quadrant, for the case $r_2 \leq r_1k$, the slow subsystem has no co-existence equilibrium; and for the case $r_2 > r_1k$, the slow subsystem (2.12) admits one unique co-existence equilibrium $E_*(\frac{r_2-r_1k}{r_1+b_1r_2}, \frac{1+b_1k}{r_1+b_1r_2})$.

We analyze linear stability of the co-existence equilibrium when $r_2 > r_1k$. The Jacobian matrix of the slow subsystem (2.12) restricted to $E_*(\frac{r_2-r_1k}{r_1+b_1r_2}, \frac{1+b_1k}{r_1+b_1r_2})$ is as follows

$$J(E_*) = \begin{pmatrix} -\frac{a_1b_1(r_2-r_1k)}{r_1+b_1r_2} & -\frac{a_1r_1(r_2-r_1k)}{r_1+b_1r_2}\\ \frac{a_2}{r_2} & -a_2\end{pmatrix}.$$

Then the determinant and trace of $J(E_*)$ are

$$\begin{aligned}\det(J(E_*)) &= \frac{a_1a_2(b_1r_2+r_1)(r_2-r_1k)}{r_2(r_1+b_1r_2)} > 0,\\ \operatorname{tr}(J(E_*)) &= -\frac{a_1b_1(r_2-r_1k)}{r_1+b_1r_2} - a_2 < 0.\end{aligned}$$

Therefore, the co-existence equilibrium $E_*(\frac{r_2-r_1k}{r_1+b_1r_2}, \frac{1+b_1k}{r_1+b_1r_2})$ is stable. □

**Remark 2.7.** Since the equilibrium $E_2$ is a high-order equilibrium when $r_2 = r_1k$, for the slow subsystem (2.12), the investigation of the dynamics in a small neighbourhood of $E_2$ is challenging. We leave the case for future study.

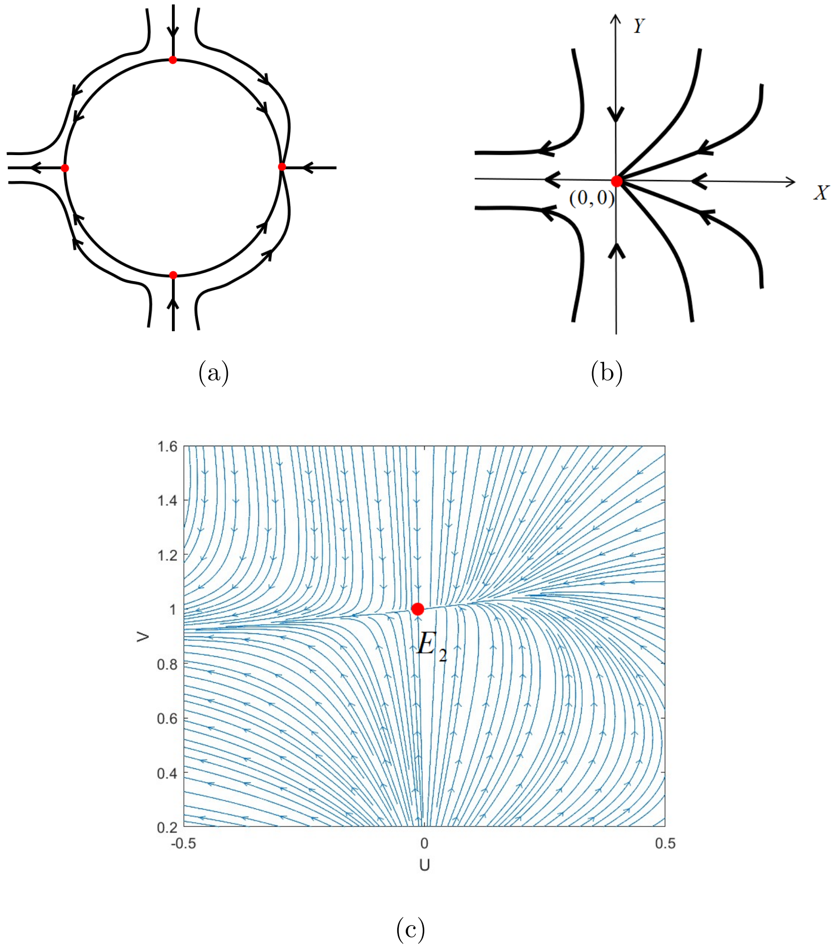


Figure 1. (a) Diagram depicting the dynamics after the blow-up at $(0,0)$, (b) trajectory distribution near $(0,0)$, (c) phase portrait of the system (2.12) around $E_2$ with $a_1 = a_2 = 2$, $b_1 = r_1 = 1$, $r_2 = 5$ and $k = 5$.

## 3. Heteroclinic orbits of the slow subsystem (2.12)

In this section, we explore the existence of heteroclinic orbits for the slow subsystem (2.12). Based on Lemma 2.6, the existence results are divided into two cases.

**Case 1:** When $r_2 < r_1 k$, the slow subsystem (2.12) has no co-existence equilibrium. In this case, we respectively demonstrate the existence of heteroclinic orbits from $E_0$ to $E_2$ and from $E_1$ to $E_2$ in Section 3.1, as shown in Theorem 3.3.

**Case 2:** When $r_2 > r_1 k$, the slow subsystem (2.12) possesses a unique co-existence equilibrium $E_*$. In this case, we have the existence of heteroclinic orbits between $E_0$, $E_1$, $E_2$ and $E_*$ in Section 3.2, as shown in Theorem 3.5.

3.1. **Existence of heteroclinic orbits for the slow subsystem** (2.12) **without co-existence equilibrium.** From Lemma 2.5 and Lemma 2.6, we determine that if $r_2 < r_1 k$, the slow subsystem (2.12) only possesses three boundary equilibria $E_0(0,0)$, $E_1(\frac{1}{b_1}, 0)$ and $E_2(0, \frac{k}{r_2})$. Moreover, $E_0$ is an unstable node, $E_1$ is a saddle, and $E_2$ is a stable node. From the phase portrait shown in Figure 2, we find that there are two different types of orbits connecting $E_0(0,0)$ to $E_2(0, \frac{k}{r_2})$ and $E_1(\frac{1}{b_1}, 0)$ to $E_2(0, \frac{k}{r_2})$.

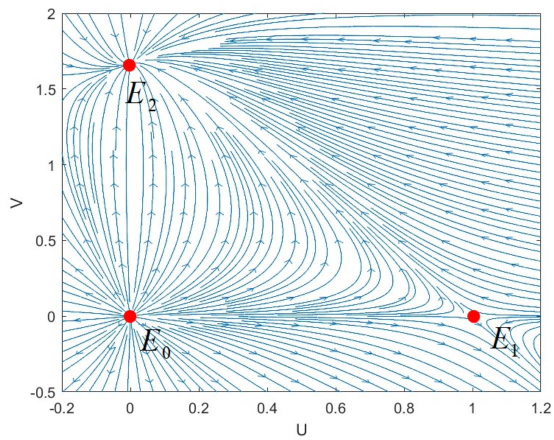


FIGURE 2. Phase portrait of the system (2.12) with $a_1 = a_2 = 2$, $b_1 = r_1 = 1$, $r_2 = 3$ and $k = 5$.

We define the region $\Omega_1 \in \mathbf{R}^2$ as

$$\Omega_1 = \{(U,V) : 0 \le U \le \frac{1}{b_1}, 0 \le V \le \frac{b_1 k + 1}{b_1 r_2}\},$$

which is displayed in Figure 3 (a).

**Lemma 3.1.** *If $r_2 < r_1 k$, then $\Omega_1$ is a positively invariant region of the slow subsystem* (2.12).

*Proof.* The region $\Omega_1$ is surrounded by four lines

$$\Gamma_1 = \{(U,V)|U = 0, 0 \le V \le \frac{b_1 k + 1}{b_1 r_2}\},$$

$$\Gamma_2 = \{(U,V)|V = 0, 0 \le U \le \frac{1}{b_1}\},$$

$$\Gamma_3 = \{(U,V)|U = \frac{1}{b_1}, 0 \le V \le \frac{b_1 k + 1}{b_1 r_2}\},$$

$$\Gamma_4 = \{(U,V)|V = \frac{b_1 k + 1}{b_1 r_2}, 0 \le U \le \frac{1}{b_1}\}.$$

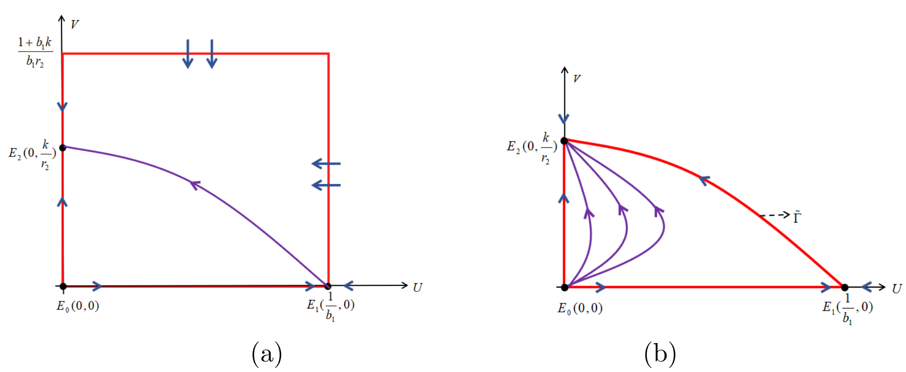


FIGURE 3. Schematic of invariant regions for system (2.12) with $r_2 < r_1 k$, where $\Omega_1$ in (a), and $\Omega_2$ in (b).

We shall demonstrate that no trajectory of the slow subsystem (2.12) initiated within the region $\Omega_1$ can leave $\Omega_1$ through the boundaries $\Gamma_i (i = 1, 2, 3, 4)$. This indicates that for any point

$(U,V) \in \Gamma_i (i = 1,2,3,4)$, it satisfies the condition

$$\mathbf{n}_i \cdot (\dot{U}, \dot{V})\big|_{\Gamma_i} \le 0,$$

where $\mathbf{n}_i$ indicates the outward normal vector of $\Gamma_i$ at the point $(U,V)$. It is obvious that $\Gamma_1$ and $\Gamma_2$ are both invariant sets of system (2.12) and no trajectories of (2.12) can intersect the boundaries $\Gamma_1$ or $\Gamma_2$.

The boundary $\Gamma_3$ has the outer normal vector $\mathbf{n_3} = (1,0)$. Then for all points $(U,V) \in \Gamma_3$, we find that

$$\mathbf{n}_3 \cdot (\dot{U}, \dot{V}) \mid_{\Gamma_3} = -\frac{a_1 r_1}{b_1} V \le 0.$$

The boundary $\Gamma_4$ has the outer normal vector written as $\mathbf{n_4} = (0,1)$. For any point $(U,V) \in \Gamma_4$, we have

$$\mathbf{n}_4 \cdot (\dot{U}, \dot{V}) \mid_{\Gamma_4} = \frac{a_2(b_1 k + 1)(b_1 U - 1)}{{b_1}^2 r_2 (U + k)} \le 0.$$

Thus, the direction of the vector field along the boundaries $\Gamma_3$ and $\Gamma_4$ points into $\Omega_1$. It follows that no orbits of the slow subsystem (2.12) can leave the boundaries $\Gamma_i$, $i = 1,2,3,4$.

The proof is complete. The invariant region $\Omega_1$, which is surrounded by four red lines, with arrows indicating the flow direction along the boundaries is shown in Figure 3 (a). □

Subsequently, we prove that the unstable manifold of $E_1(\frac{1}{b_1}, 0)$ starting from $E_1$ will enter the region $\Omega_1$.

**Lemma 3.2.** *The unstable manifold emanating from $E_1(\frac{1}{b_1}, 0)$ of the slow subsystem* (2.12) *will intersect the region $\Omega_1$, that is $W_u(E_1) \cap \Omega_1 \ne \emptyset$.*

*Proof.* According to Lemma 2.5, the linearization matrix at $E_1$ has two different eigenvalues $-a_1 < 0$ and $a_2 > 0$. Consequently, the boundary equilibrium $E_1$ possesses a one-dimensional stable manifold and a one-dimensional unstable manifold. The stable manifold approaches $E_1$ along the U-axis. The local unstable manifold of $E_1$ is tangential to $\varsigma$, which is the corresponding eigenvector of the positive eigenvalue $a_2$ and reads as

$$\varsigma := (-1, \frac{(a_1 + a_2) b_1}{a_1 r_1})^T.$$

Thus $W_u(E_1) \cap \Omega_1 \ne \emptyset$, for the slope of $\varsigma$ is $-\frac{(a_1+a_2)b_1}{a_1 r_1} < 0$. □

Using Lemmas 3.1 and 3.2, we obtain the existence of heteroclinic orbits between $E_0$, $E_1$ and $E_2$ for the slow subsystem (2.12).

**Theorem 3.3.** *If $r_2 < r_1 k$, then the following statements hold.*

- (i) *The slow subsystem* (2.12) *has a unique heteroclinic orbit $(U,V)$ connecting the equilibrium $E_1(\frac{1}{b_1}, 0)$ to $E_2(0, \frac{k}{r_2})$.*
- (ii) *The slow subsystem* (2.12) *has infinite number of heteroclinic orbits $(U,V)$ that connects the equilibrium $E_0(0,0)$ to $E_2(0, \frac{k}{r_2})$.*

*Proof.* (i) We denote

$$P(U,V) = a_1 U(1 - b_1 U - r_1 V), \quad Q(U,V) = a_2 V(1 - \frac{r_2 V}{U + k}).$$

Assume that there exists a closed orbit $\mathfrak{L}$ within the region $\Omega_1$. The rotation number of the closed orbit $\mathfrak{L}$ with respect to the vector field $(P,Q)$ is 1. In fact, the rotation number of $\mathfrak{L}$ with respect to the vector field $(P,Q)$ must be 0 due to no equilibrium in $\Omega_1$, which leads to a contradiction. This implies that if there exists a closed orbit, its interior must contain at least one equilibrium. Therefore, it is evident that the slow subsystem (2.12) has no closed orbit in $\Omega_1$. Our discussion for the type of equilibria in Lemma 2.5 reveals that $E_1$ is a saddle, characterized by a one-dimensional unstable manifold. Furthermore, Lemma 3.2 indicates that the unstable manifold will enter $\Omega_1$. Therefore, according to the Poincaré-Bendixson theorem, the $\omega$ limit of the unstable manifold of $E_1$ in $\Omega_1$ is identified as $E_2$. Consequently, the slow subsystem (2.12) admits a unique heteroclinic orbit connecting $E_1$ to $E_2$, which is denoted by $\tilde{\Gamma}$.

(ii) We define a region $\Omega_2$, which is bounded by two segments $\Gamma_2$, $E_0E_2$ and the orbit $\tilde{\Gamma}$. Figure 3 (b) displays $\Omega_2$ with red curves, with arrows indicating the flow direction on the boundary. Since $\Gamma_2$, $\tilde{\Gamma}$ and $E_0E_2$ are all orbits of the slow subsystem (2.12), it is clear that $\Omega_2$ is invariant as orbits cannot intersect. All equilibria in this region are located on the boundaries, hence the slow subsystem (2.12) does not have any closed orbit in $\Omega_2$. Based on Lemma 2.5, we know that $E_0$ is an unstable node which is repelling, while $E_2$ is a stable node which is attracting. Therefore, by applying the Poincaré-Bendixson theorem, the slow subsystem (2.12) possesses infinitely many heteroclinic orbits connecting the equilibria $E_0$ and $E_2$. □

A numerical simulation to illustrate Theorem 3.3 is presented in Figure 4.

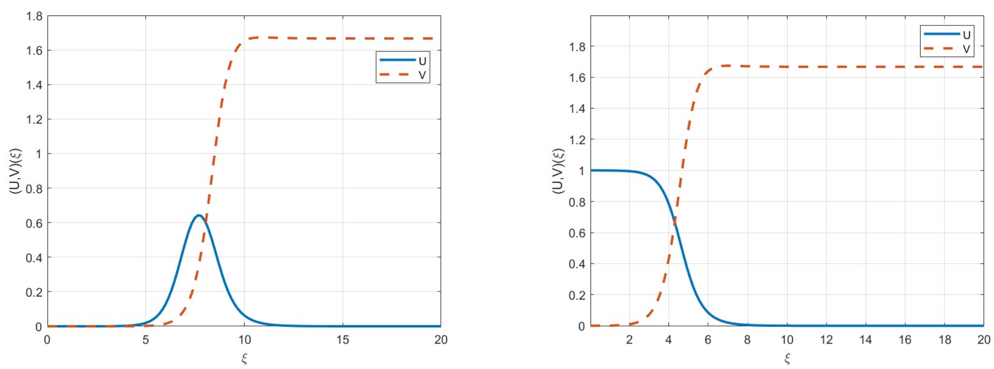


FIGURE 4. Numerical simulation diagrams of two types of heteroclinic orbits, as described in Theorem 3.3, generated from system (2.12) with different initial values, where $a_1 = a_2 = 2$, $b_1 = r_1 = 1$, $r_2 = 3$ and $k = 5$.

3.2. **Existence of heteroclinic orbits for the slow subsystem** (2.12) **with a unique co-existence equilibrium** $E_*$**.** Based on Lemma 2.5 and Lemma 2.6, when $r_2 > r_1k$, the slow subsystem (2.12) has a unique co-existence equilibrium $E_*(\frac{r_2-r_1k}{r_1+b_1r_2}, \frac{1+b_1k}{r_1+b_1r_2})$ and three boundary equilibria $E_0(0,0)$, $E_1(\frac{1}{b_1},0)$, $E_2(0,\frac{k}{r_2})$. Among them, $E_0$ is an unstable node, $E_1$ and $E_2$ are two saddles, and co-existence equilibrium $E_*$ is stable. As depicted in Figure 5, the phase portrait of system (2.12) reveals that there exist three distinct types of heteroclinic orbits. Subsequently, we shall present a detailed demonstration.

From
$$P(U,V) = a_1U(1 - b_1U - r_1V), \quad Q(U,V) = a_2V(1 - \frac{r_2V}{U+k}),$$
we obtain
$$\begin{aligned}
(P_U + Q_V)|_{U_*} &= a_1(1 - 2b_1U_* - r_1V_*) + a_2(1 - \frac{2r_2V_*}{U_*+k}) \\
&= a_1(1 - 2b_1\frac{r_2 - r_1k}{r_1 + b_1r_2} - r_1\frac{1 + b_1k}{r_1 + b_1r_2}) \\
&\quad + a_2[1 - \frac{2r_2(r_1 + b_1r_2)}{r_2 - r_1k + k(r_1 + b_1r_2)}\frac{1 + b_1k}{r_1 + b_1r_2}] \\
&= -\frac{a_1b_1(r_2 - r_1k)}{r_1 + b_1r_2} - a_2 < 0.
\end{aligned}$$
Therefore, the sign of $P_U + Q_V$ remains unchanged within a sufficiently small neighborhood of $E_*$. According to Dulac theorem, there is no closed orbits in this neighborhood. Moreover, since $E_*$ is locally stable, the trajectory originating from the point $(\frac{r_2-r_1k}{r_1+b_1r_2} + \epsilon, \frac{1+b_1k}{r_1+b_1r_2} + \epsilon)$ must converge to $E_*$, where the constant $\epsilon$ is sufficiently small. We denote this trajectory by $\hat{L}$.

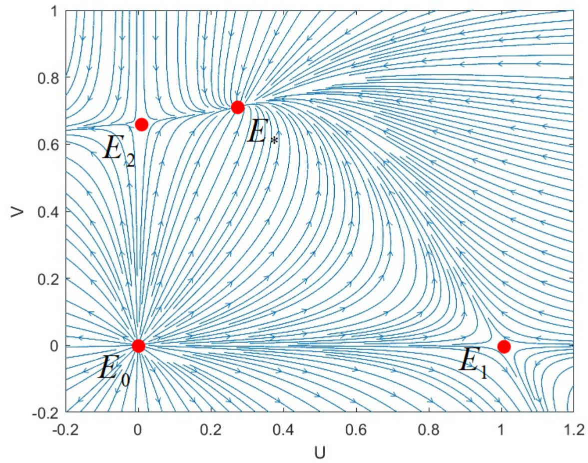


FIGURE 5. Phase portrait of the system (2.12) with $a_1 = a_2 = 2$, $b_1 = r_1 = 1$, $r_2 = 6$ and $k = 4$.

Furthermore, for $b_1U + r_1V - 1 \geq 0$, if $U \geq U_*$, we obtain

$$\begin{aligned}
b_1\dot{U} + r_1\dot{V} &= r_1a_2V(1 - \frac{r_2}{U+k}\frac{1-b_1U}{r_1}) \\
&= \frac{a_2V}{U+k}[(r_1 + r_2b_1)U + r_1k - r_2] \\
&\geq \frac{a_2V}{U+k}[(r_1 + r_2b_1)\frac{r_2 - r_1k}{r_1 + b_1r_2} + r_1k - r_2] \\
&= \frac{a_2V}{U+k}(r_2 - r_1k + r_1k - r_2) = 0.
\end{aligned}$$

Thus, for the trajectory $\hat{L}$, we have $\dot{U} \leq 0$, that is the $U$-component of $\hat{L}$ is monotonically decreasing.

Similarly, for $r_2V - U - k \geq 0$, if $U \geq U_*$, we obtain

$$\begin{aligned}
r_2\dot{V} - \dot{U} &= -a_1U(1 - b_1U - r_1V) \\
&= -a_1U(1 - b_1U - r_1\frac{U+k}{r_2}) \\
&= \frac{a_1U}{r_2}[(r_1 + b_1r_2)U + (r_1k - r_2)] \\
&\geq \frac{a_1U}{r_2}[(r_1 + b_1r_2)\frac{r_2 - r_1k}{r_1 + b_1r_2} + (r_1k - r_2)] \\
&= \frac{a_1U}{r_2}(r_2 - r_1k + r_1k - r_2) = 0.
\end{aligned}$$

Then, for the trajectory $\hat{L}$, we have $\dot{V} \leq 0$, that is the $V$-component of $\hat{L}$ is monotonically decreasing.

Consequently, there exists $\hat{\xi} \in \mathbf{R}$ such that the trajectory $\hat{L}$ intersects the line $U = \frac{1}{b_1}$ at a point $\phi_{\hat{\xi}}(\frac{r_2 - r_1k}{r_1 + b_1r_2} + \epsilon, \frac{1 + b_1k}{r_1 + b_1r_2} + \epsilon) = \hat{P}(\frac{1}{b_1}, \hat{a})$ as $\xi \to -\infty$. Then, we have the following lemma.

**Lemma 3.4.** *If $r_2 > r_1k$, then the region $\Sigma_1$ is a positively invariant region for the slow subsystem* (2.12).

*Proof.* We define a region $\Sigma_1 \in \mathbf{R}^2$, which is bounded by three segments and a trajectory $L_i$ $(i = 1, 2, 3, 4)$, where

$$L_1 := \{(U,V)|U = \frac{r_2 - r_1 k}{r_1 + b_1 r_2}, 0 \le V \le \frac{b_1 k + 1}{r_1 + b_1 r_2}\},$$
$$L_2 := \{(U,V)|V = 0, \frac{r_2 - r_1 k}{r_1 + b_1 r_2} \le U \le \frac{1}{b_1}\},$$
$$L_3 := \{(U,V)|U = \frac{1}{b_1}, 0 \le V \le \hat{a}\},$$
$$L_4 := \{(U,V)|\phi_\xi(\frac{r_2 - r_1 k}{r_1 + b_1 r_2} + \epsilon, \frac{1 + b_1 k}{r_1 + b_1 r_2} + \epsilon), \xi \in [\hat{\xi}, +\infty)\}.$$

The outer normal vector of $L_1$ is $\mathbf{N_1} = (-1, 0)$. For any point $(U,V) \in L_1$, we have

$$\begin{aligned}\mathbf{N_1} \cdot (\dot{U}, \dot{V})|_{L_1} &= -a_1 \frac{r_2 - r_1 k}{r_1 + b_1 r_2}(1 - b_1 \frac{r_2 - r_1 k}{r_1 + b_1 r_2} - r_1 V) \\ &\le \frac{r_2 - r_1 k}{r_1 + b_1 r_2}(1 - b_1 \frac{r_2 - r_1 k}{r_1 + b_1 r_2} - r_1 \frac{1 + b_1 k}{r_1 + b_1 r_2}) = 0.\end{aligned}$$

Based on Lemma 3.1, no trajectory of the slow subsystem (2.12) can leave through the boundaries $L_2$ and $L_3$. Therefore, any trajectory of the slow subsystem (2.12) starting inside $\Sigma_1$ cannot leave $\Sigma_1$ through its boundaries $L_i$ $(i = 1, 2, 3)$. Since $L_4$ is a trajectory of the slow subsystem (2.12) and trajectories cannot intersect, $\Sigma_1$ is a positively invariant region.

The proof is complete. A schematic of $\Sigma_1$ is shown in Figure 6 (a), where the flow directions along boundaries are marked by arrows. $\square$

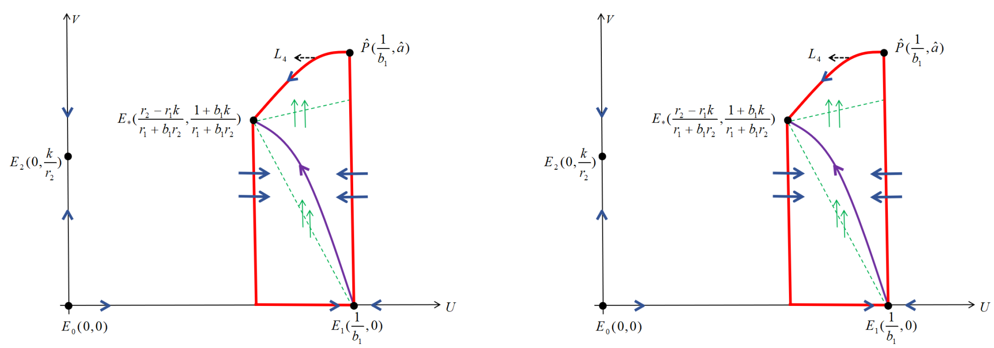


(a) (b)

FIGURE 6. Schematic of invariant regions for system (2.12) with $r_2 > r_1 k$, where $\Sigma_1$ in (a), and $\Sigma_2$ in (b).

The slow subsystem (2.12) admits heteroclinic orbits connecting between the equilibria $E_0(0,0)$, $E_1(\frac{1}{b_1}, 0)$, $E_2(0, \frac{k}{r_2})$, and $E_*(\frac{r_2 - r_1 k}{r_1 + b_1 r_2}, \frac{1 + b_1 k}{r_1 + b_1 r_2})$, which can be stated as follows.

**Theorem 3.5.** *If $r_2 > r_1 k$, then the following statements hold.*

- (i) *the slow subsystem* (2.12) *has a single heteroclinic orbit that connects the equilibrium $E_1(\frac{1}{b_1}, 0)$ to $E_*(\frac{r_2 - r_1 k}{r_1 + b_1 r_2}, \frac{1 + b_1 k}{r_1 + b_1 r_2})$.*
- (ii) *the slow subsystem* (2.12) *has infinitely many heteroclinic orbits connecting the equilibrium $E_0(0,0)$ to $E_*(\frac{r_2 - r_1 k}{r_1 + b_1 r_2}, \frac{1 + b_1 k}{r_1 + b_1 r_2})$.*
- (iii) *the slow subsystem* (2.12) *has a unique heteroclinic orbit connecting the equilibrium $E_2(0, \frac{k}{r_2})$ to $E_*(\frac{r_2 - r_1 k}{r_1 + b_1 r_2}, \frac{1 + b_1 k}{r_1 + b_1 r_2})$.*

*Proof.* (i) Since there is no equilibrium inside $\Sigma_1$, it is evident that the slow subsystem (2.12) cannot have a closed orbit in $\Sigma_1$. By applying the Poincaré-Bendixson theorem, any trajectory starting from the unstable manifold of $E_1$ must eventually approach the stable co-existence equilibrium $E_*$. Hence, the slow subsystem (2.12) features a heteroclinic orbit connecting $E_1$ to $E_*$. Additionally, it follows that $E_1$ possesses a one-dimensional unstable manifold, therefore this heteroclinic orbit is unique, and we denote it by $\tilde{L}$.

(ii) Define the region $\Sigma_2$ as the area enclosed by three segments $\Gamma_2$, $E_0A$, $E_*A$ and one orbit $\tilde{L}$, which is shown in Figure 6 (b). According to Lemma 3.1, the trajectories can not leave $\Sigma_2$ from the segments $\Gamma_2$ and $E_0A$. Additionally, the outwards vector of $E_*A$ is written by $\mathbf{N_{E_*A}} = (0, 1)$. For all points $(U, V) \in N_{E_*A}$, one has

$$\begin{aligned} \mathbf{N_{E_*A}} \cdot (\dot{U}, \dot{V}) &= a_2 \frac{b_1k+1}{r_1+b_1r_2}\big[1 - \frac{r_2(b_1k+1)}{(U+k)(r_1+b_1r_2)}\big] \\ &\leq a_2 \frac{b_1k+1}{r_1+b_1r_2}[1 - \frac{r_2(b_1k+1)(r_1+b_1r_2)}{(r_2+b_1r_2k)(r_1+b_1r_2)}] = 0. \end{aligned}$$

Since orbits cannot intersect, it is evident that $\Sigma_2$ is a positively invariant region for the slow subsystem (2.12). All equilibria lie on the boundaries. Hence, the slow subsystem (2.12) does not possess any closed orbits within $\Sigma_2$. Drawing from Lemma 2.5 and Lemma 2.6, we recognize that $E_0$ is repelling, while $E_*$ is attracting. Consequently, applying the the Poincaré-Bendixson theorem, the slow subsystem (2.12) contains an infinite number of heteroclinic orbits that connect the equilibria $E_0$ and $E_*$.

(iii) Since $E_2$ is a saddle when $r_2 > r_1k$, the equilibrium $E_2$ of system (2.12) has a one-dimensional unstable manifold. Through a straightforward calculation, we know that the eigenvector $\nu$ of the Jacobian matrix $J(E_2)$ is $(1, \frac{a_2}{a_1(r_2-r_1k)+a_2r_2})^T$, which is directed towards the interior of the region $\Sigma_2$. Therefore, the unstable manifold of $E_2$ tangent to $\nu$ will enter $\Sigma_2$. Applying Poincaré-Bendixson theorem, there exists only one heteroclinic orbit from $E_2$ to $E_*$.

The proof is complete. A numerical simulation demonstrating the heteroclinic orbits of the slow subsystem (2.12) is shown in Figure 7. □

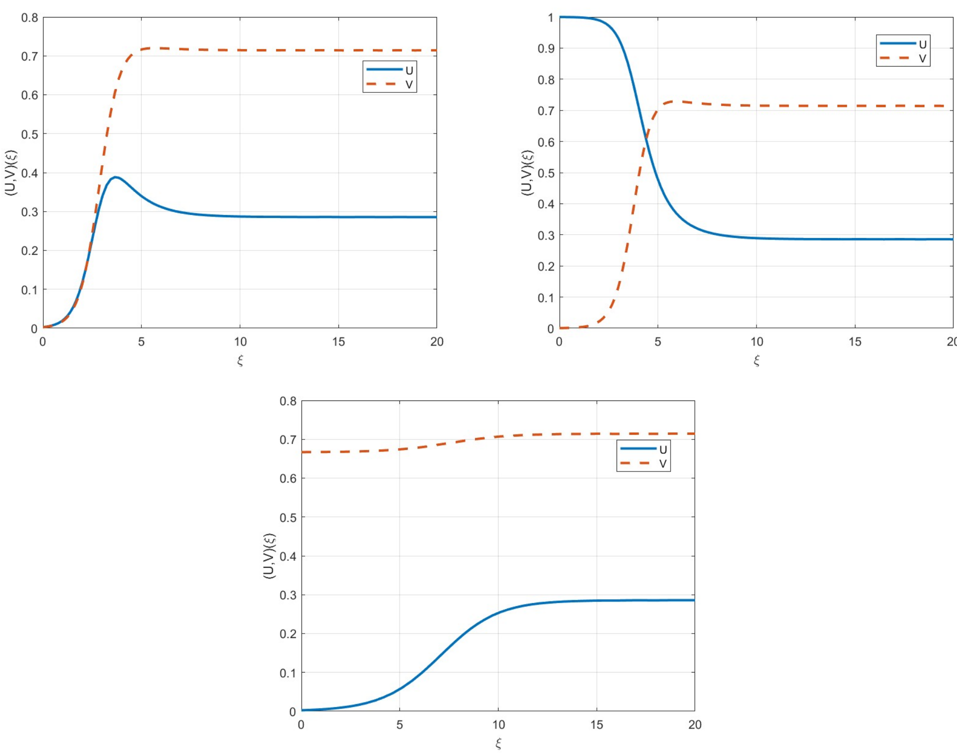


FIGURE 7. Numerical simulation diagrams of three types of heteroclinic orbits, as described in Theorem 3.5, where $a_1 = a_2 = 2$, $b_1 = r_1 = 1$, $r_2 = 6$ and $k = 2$.

## 4. Traveling wave solutions of system (1.5)

In this section, we focus on investigating the presence of traveling wave solution for system (1.5) with the large wave speed. This problem is equivalent to studying the heteroclinic orbits for the slow system (2.8). The main tools we use are the geometric singular perturbation theory and Fredholm theory.

Referring to Lemma 2.3, we have that there admits a slow manifold $M_\varepsilon$, which is $\mathcal{O}(\varepsilon)$-close to $M_0$ for sufficiently small $\varepsilon > 0$. Furthermore, $M_\varepsilon$ and $M_0$ are diffeomorphic.

The slow manifold $M_\varepsilon$ can be expressed as

$$M_\varepsilon = \big\{(U, U_1, V, V_1) : U_1 = P(U, V) + \bar{\phi}(U, V, \varepsilon), \quad V_1 = Q(U, V) + \bar{\psi}(U, V, \varepsilon)\big\},$$

where

$$P(U, V) = a_1 U(1 - b_1 U - r_1 V), \quad Q(U, V) = a_2 V(1 - \frac{r_2 V}{U + k}),$$

$\bar{\phi}$ and $\bar{\psi}$ are both smooth functions of $\varepsilon$ that satisfy

$$\bar{\phi}(U, V, 0) = 0 \quad \text{and} \quad \bar{\psi}(U, V, 0) = 0.$$

Thus these functions $\bar{\phi}$ and $\bar{\psi}$ can be expanded in a Taylor series with respect to the $\varepsilon$ as follows

$$\begin{aligned}
\bar{\phi}(U, V, \varepsilon) &= \varepsilon\phi_1(U, V, \varepsilon) + \mathcal{O}(\varepsilon^2),\\
\bar{\psi}(U, V, \varepsilon) &= \varepsilon\psi_1(U, V, \varepsilon) + \mathcal{O}(\varepsilon^2).
\end{aligned}$$

By substituting

$$\begin{aligned}
U_1 &= P(U, V) + \bar{\phi}(U, V, \varepsilon),\\
V_1 &= Q(U, V) + \bar{\psi}(U, V, \varepsilon),
\end{aligned}$$

into the slow system (2.8), we obtain

$$\begin{aligned}
\varepsilon\dot{U}_1 &= \varepsilon(\frac{\partial U_1}{\partial U}\dot{U} + \frac{\partial U_1}{\partial V}\dot{V})\\
&= \varepsilon\Big[(P_U + \varepsilon\phi_{1U})\dot{U} + (P_V + \varepsilon\phi_{1V})\dot{V}\Big] + \mathcal{O}(\varepsilon^2)\\
&= \varepsilon(P_U U_1 + P_V V_1) + \mathcal{O}(\varepsilon^2),
\end{aligned}$$

and

$$\begin{aligned}
\varepsilon\dot{V}_1 &= \varepsilon(\frac{\partial V_1}{\partial U}\dot{V} + \frac{\partial V_1}{\partial V}\dot{V})\\
&= \varepsilon\Big[(Q_U + \varepsilon\psi_{1U})\dot{U} + (Q_V + \varepsilon\psi_{1V})\dot{V}\Big] + \mathcal{O}(\varepsilon^2)\\
&= \varepsilon(Q_U U_1 + Q_V V_1) + \mathcal{O}(\varepsilon^2),
\end{aligned}$$

where

$$\begin{gathered}
P_U = a_1(1 - 2b_1 U - r_1 V), \quad P_V = -a_1 r_1 U,\\
Q_U = \frac{a_2 r_2 V^2}{(U + k)^2}, \quad Q_V = a_2(1 - \frac{2r_2 V}{U + k}).
\end{gathered}$$

By examining the equations of the slow system (2.8), we find that

$$\begin{aligned}
\varepsilon\dot{U}_1 &= U_1 - a_1 U(1 - b_1 U - r_1 V)\\
&= a_1 U(1 - b_1 U - r_1 V) + \phi_1(U, V)\varepsilon + \mathcal{O}(\varepsilon^2) - a_1(1 - b_1 U - r_1 V)\\
&= \phi_1(U, V)\varepsilon + \mathcal{O}(\varepsilon^2),
\end{aligned}$$

and

$$\begin{aligned}
\varepsilon\dot{V}_1 &= -\varepsilon\gamma U_1 V_1 - \gamma V[U_1 - a_1 U(1 - b_1 U - r_1 V)] + \frac{1}{\rho}V_1 - \frac{a_2}{\rho}V(1 - \frac{r_2 V}{U + k})\\
&= -\varepsilon\gamma\big[a_1 U(1 - b_1 U - r_1 V) + \phi_1(U, V)\varepsilon + \mathcal{O}(\varepsilon^2)\big]\big[a_2 V(1 - \frac{r_2 V}{U + k})
\end{aligned}$$

$$
\begin{aligned}
&+ \psi_1(U,V)\varepsilon + \mathcal{O}(\varepsilon^2)\big] - \gamma V\big[a_1U(1-b_1U-r_1V) + \phi_1(U,V)\varepsilon \\
&+ \mathcal{O}(\varepsilon^2) - a_1U(1-b_1U-r_1V)\big] + \frac{1}{\rho}[a_2V(1-\frac{r_2V}{U+k}) + \psi_1(U,V)\varepsilon + \mathcal{O}(\varepsilon^2)] \\
&- \frac{a_2}{\rho}V(1-\frac{r_2V}{U+k}) \\
={}& -\varepsilon\gamma\big[a_1a_2UV(1-b_1U-r_1V)(1-\frac{r_2V}{U+k})\big] - \gamma V\phi_1(U,V)\varepsilon \\
&+ \frac{1}{\rho}\psi_1(U,V)\varepsilon + \mathcal{O}(\varepsilon^2) \\
={}& \big[-\gamma a_1a_2UV(1-b_1U-r_1V)(1-\frac{r_2V}{U+k}) - \gamma V\phi_1(U,V) \\
&+ \frac{1}{\rho}\psi_1(U,V)\big]\varepsilon + \mathcal{O}(\varepsilon^2).
\end{aligned}
$$

Comparing the coefficients of $\varepsilon$ in the above equations, we obtain

$$
\begin{gathered}
\phi_1(U,V) = P_UU_1 + P_VV_1, \\
\begin{aligned}
\psi_1(U,V) = \gamma\rho a_1a_2UV(1-b_1U-r_1V)(1-\frac{r_2V}{U+k}) + \gamma\rho V(P_UU_1 \\
+ P_VV_1) + \rho(Q_UU_1 + Q_VV_1),
\end{aligned}
\end{gathered}
$$

and

$$
\begin{aligned}
M_\varepsilon = \Big\{(U,U_1,V,V_1) : U_1 &= P(U,V) + \varepsilon(P_UU_1 + P_VV_1) + \mathcal{O}(\varepsilon^2), \\
V_1 &= Q(U,V) + \varepsilon\big[\gamma\rho a_1a_2UV(1-b_1U-r_1V)(1-\frac{r_2V}{U+k}) \\
&+ \gamma\rho V(P_UU_1 + P_VV_1) + \rho(Q_UU_1 + Q_VV_1)\big] + \mathcal{O}(\varepsilon^2)\Big\}.
\end{aligned}
$$

Then the slow system (2.8) restricted to $M_\varepsilon$ is described by

$$
\begin{aligned}
\frac{dU}{d\xi} &= a_1U(1-b_1U-r_1V) + \varepsilon(P_UU_1 + P_VV_1) + \mathcal{O}(\varepsilon^2), \\
\frac{dV}{d\xi} &= a_2V(1-\frac{r_2V}{U+k}) + \varepsilon\Big\{\gamma\rho a_1a_2UV(1-b_1U-r_1V)(1-\frac{r_2V}{U+k}) \\
&+ \gamma\rho V(P_UU_1 + P_VV_1) + \rho(Q_UU_1 + Q_VV_1)\Big\} + \mathcal{O}(\varepsilon^2).
\end{aligned} \tag{4.1}
$$

It is evident that the system (4.1) is reduced to the slow subsystem (2.12) as $\varepsilon \to 0$.

Next, we demonstrate that for $0 < \varepsilon \ll 1$, the system (4.1) admits a heteroclinic orbit connecting $E_1(\frac{1}{b_1}, 0)$ to $E_2(0, \frac{k}{r_2})$ under the condition $r_2 < r_1k$. For $\varepsilon = 0$, by Theorem 3.3, it follows that the system (4.1) has a heteroclinic orbit connecting $E_1$ to $E_2$, written as $(U_0, V_0)$.

For $0 < \varepsilon \ll 1$, we set

$$
\begin{aligned}
U &= U_0 + \varepsilon\hat{U}_1 + \dots, \\
V &= V_0 + \varepsilon\hat{V}_1 + \dots.
\end{aligned} \tag{4.2}
$$

Substituting this expansion in the system (4.1) and equating the coefficients of $\varepsilon$, we derive the differential system that determines $\hat{U}_1$ and $\hat{V}_1$

$$
\frac{d\varphi(\xi)}{d\xi} - H(\xi)\varphi(\xi) = C(\xi), \tag{4.3}
$$

where

$$
\begin{gathered}
\varphi(\xi) = \begin{pmatrix} \hat{U}_1 \\ \hat{V}_1 \end{pmatrix}, \quad H(\xi) = \begin{pmatrix} a_1(1-2b_1U_0-r_1V_0) & -a_1r_1U_0 \\ \frac{a_2r_2V_0^2}{(U_0+k)^2} & a_2(1-\frac{2r_2V_0}{U_0+k}) \end{pmatrix}, \\
C(\xi) = \begin{pmatrix} c_1 \\ c_2 \end{pmatrix},
\end{gathered}
$$

$$c_1 = {a_1}^2 U_0(1-2b_1U_0-r_1V_0)(1-b_1U_0-r_1V_0) - a_1a_2r_1U_0V_0(1-\frac{r_2V_0}{U_0+k}),$$

$$\begin{aligned}
c_2 &= \gamma\rho a_1a_2U_0V_0(1-b_1U_0-r_1V_0)(1-\frac{r_2V_0}{U_0+k}) \\
&\quad + \gamma\rho V_0\Big[{a_1}^2U_0(1-2b_1U_0-r_1V_0)(1-b_1U_0-r_1V_0) \\
&\quad - a_1a_2r_1U_0V_0(1-\frac{r_2V_0}{U_0+k})\Big] + \rho a_1a_2r_2\frac{U_0{V_0}^2}{(U_0+k)^2}(1-b_1U_0-r_1V_0) \\
&\quad + \rho {a_2}^2V_0(1-\frac{2r_2V_0}{U_0+k})(1-\frac{r_2V_0}{U_0+k}).
\end{aligned}$$

Subsequently, we demonstrate that system (4.3) admits a solution that satisfies the boundary condition

$$\hat{U}_1(\pm\infty) = 0,\ \hat{V}_1(\pm\infty) = 0.$$

We define the operator

$$\mathcal{L} = \frac{d}{d\xi} - H(\xi),$$

and let $L^2$ represent the space of square-integrable functions, with inner production given by

$$\int_{-\infty}^{+\infty}(X(\xi), N(\xi))d\xi,$$

where the notation $(\cdot,\cdot)$ denotes the Euclidean inner product on $\mathbf{R}^2$. According to the Fredholm theory, the system (4.3) has a solution if and only if

$$\int_{-\infty}^{+\infty}(X(\xi), C(\xi))d\xi = 0,$$

for all functions $X(\xi) \in \mathbf{R}^2$ that lie in the kernel of the adjoint operator $\mathcal{L}$. It can be easily confirmed that the adjoint operator $\mathcal{L}^*$ is given by

$$\mathcal{L}^* = -\frac{d}{d\xi} - H^T(\xi),$$

where

$$H^T(\xi) = \begin{pmatrix} a_1(1-2b_1U_0-r_1V_0) & \frac{a_2r_2{V_0}^2}{(U_0+k)^2} \\ -a_1r_1U_0 & a_2(1-\frac{2r_2V_0}{U_0+k}) \end{pmatrix}.$$

To determine the kernel of $\mathcal{L}^*$, we should seek all $X(\xi)$ satisfying $\mathcal{L}^*X(\xi) = 0$, that is,

$$\frac{dX(\xi)}{d\xi} = -H^T(\xi)X(\xi). \tag{4.4}$$

Then the question of persistence reduces to the solvability of the equation (4.4). It is clear that the zero solution is a solution to equation (4.4). Since the matrix $H^T(\xi)$ is nonconstant, it is challenging to find the general solution to equation (4.4). However, we are specifically interested in solutions that meet the boundary condition $X(\pm\infty) = 0$, and indeed, the sole such solution is the zero solution. Recall that $(U_0(\xi), V_0(\xi))$ is the solution of the system (2.12) derived in Theorem 3.3. Although we do not have an explicit expression for it, it follows that $(U_0(\xi), V_0(\xi))$ tends to $E_2(0, \frac{k}{r_2})$ as $\xi \to +\infty$. As $\xi \to +\infty$, the matrix $-H^T(\xi)$ finally becomes a constant matrix

$$J^T = \begin{pmatrix} -a_1(1-\frac{r_1k}{r_2}) & 0 \\ -\frac{a_2}{r_2} & a_2 \end{pmatrix}. \tag{4.5}$$

Through a direct computation, we find the matrix $J$ admits two positive real eigenvalues $\lambda_1 = -a_1(1-\frac{r_1k}{r_2})$ and $\lambda_2 = a_2$. As a result, the only solution that meets $X(+\infty) = 0$ is the zero solution. This implies that the Fredholm orthogonality condition holds trivially

$$\int_{-\infty}^{+\infty}(X(\xi), C(\xi))d\xi = \int_{-\infty}^{+\infty}(0, C(\xi))d\xi = 0,$$

and the system (4.4) exists a solution satisfying the boundary condition

$$\hat{U}_1(\pm\infty) = 0,\ \hat{V}_1(\pm\infty) = 0.$$

Therefore, for sufficiently small $\varepsilon > 0$, the system (4.1) has a heteroclinic orbit that connects $E_1(\frac{1}{b_1}, 0)$ to $E_2(0, \frac{k}{r_2})$. For system (4.1) with $0 < \varepsilon \ll 1$, the existence of the heteroclinic orbits connecting from $E_0(0,0)$ to $E_2(0, \frac{k}{r_2})$, as well as the existence of the heteroclinic orbit linking $E_0(0,0)$, $E_1(\frac{1}{b_1}, 0)$ and $E_2(0, \frac{k}{r_2})$ to $E_*(\frac{r_2 - r_1 k}{r_1 + b_1 r_2}, \frac{1 + b_1 k}{r_1 + b_1 r_2})$, can be established in a similar way. Consequently, we get the following theorem.

**Theorem 4.1.** *There exists a large wave speed $c^* > 0$. Under the assumption $c > c^*$, with regard to the traveling waves $(U, V)(z) = (u, v)(x, t)$ of system* (1.5)*, where $z = x - ct$, the following results hold.*

(i) *If $r_2 > r_1 k$, then the system* (1.5) *has two types of traveling waves. The first type connects the equilibria $E_1(\frac{1}{b_1}, 0)$ and $E_2(0, \frac{k}{r_2})$. The second type connects $E_0(0,0)$ and $E_2(0, \frac{k}{r_2})$.*

(ii) *If $r_2 < r_1 k$, then the system* (1.5) *has three types of traveling waves. The first type connects $E_0(0,0)$ and $E_*(\frac{r_2 - r_1 k}{r_1 + b_1 r_2}, \frac{1 + b_1 k}{r_1 + b_1 r_2})$. The second type connects $E_1(\frac{1}{b_1}, 0)$ and $E_*(\frac{r_2 - r_1 k}{r_1 + b_1 r_2}, \frac{1 + b_1 k}{r_1 + b_1 r_2})$. The third type connects $E_2(0, \frac{k}{r_2})$ and $E_*(\frac{r_2 - r_1 k}{r_1 + b_1 r_2}, \frac{1 + b_1 k}{r_1 + b_1 r_2})$.*

## 5. Conclusion

In this article, we studied a diffusive modified Leslie-Gower model with chemotaxis (1.5), in which the diffusion of the predator is also influenced by prey. Through our research, it is revealed that for a large sufficiently wave speed $c > 0$, there exist five kinds of traveling waves for the system (1.5). These traveling waves of the diffusive modified Leslie-Gower model with chemotaxis (1.5) are associated with the heteroclinic orbits of the slow subsystem (2.12). In Section 3, for the slow subsystem without co-existence equilibrium, we established the existence of heteroclinic orbits connecting $E_0(0,0)$ and $E_2(0, \frac{k}{r_2})$, $E_1(\frac{1}{b_1}, 0)$ and $E_2(0, \frac{k}{r_2})$, as detailed in Theorem 3.3. For the slow subsystem with one unique co-existence equilibrium, we obtained that the existence of heteroclinic orbits connecting $E_0(0,0)$ and $E_*(\frac{r_2 - r_1 k}{r_1 + b_1 r_2}, \frac{1 + b_1 k}{r_1 + b_1 r_2})$, $E_1(\frac{1}{b_1}, 0)$ and $E_*(\frac{r_2 - r_1 k}{r_1 + b_1 r_2}, \frac{1 + b_1 k}{r_1 + b_1 r_2})$, $E_2(0, \frac{k}{r_2})$ and $E_*(\frac{r_2 - r_1 k}{r_1 + b_1 r_2}, \frac{1 + b_1 k}{r_1 + b_1 r_2})$, as shown in Theorem 3.5. To prove the existence of homoclinic orbits, we adopted the method of invariant regions and Poincaré-Bendixson theorem. In Section 4, based on the geometric singular perturbation theory and Fredholm theorem, we proved that the diffusive modified Leslie-Gower model with chemotaxis (1.5) admits the different traveling waves for $0 < \varepsilon \ll 1$. The results are demonstrated in Theorem 4.1.

**Acknowledgements.** The authors wish to thank to the anonymous referees for their valuable comments and helpful suggestions that improved the quality of this article. This work was supported by the Natural Science Foundation of China (Grant No. 12271220) and by the Postgraduate Research and Practice Innovation Program of Jiangsu Province (Grant No. KYCX24-3010).

## References

[1] M. Aziz-Alaoui, M. Okiye; Boundedness and global stability for a predator-prey model with modified Leslie-Gower and Holling-type II schemes, *Appl. Math. Lett.*, **16** (2003) 1069-1075.

[2] S. Biswas, L. Bhutia, T. Kar, et al.; patiotemporal analysis of a modified Leslie-Gower model with cross-diffusion and harvesting, *Phys. D*, **470** (2024) 134381.

[3] S. Chen, J. Li, Singular perturbations of generalized Holling type III predator-prey models with two canard points, *J. Differential Equations*, **371** (2024) 116-150.

[4] Y. Du, S. Hsu; A diffusive predator-prey model in heterogeneous environment, *J. Differential Equations*, **203** (2004) 331-364.

[5] Z. Du, J. Li, X. Li; The existence of solitary wave solutions of delayed Camassa-Holm equation via a geometric approach, *J. Funct. Anal.*, **306** (2018) 988-1007.

[6] Z. Du, J. Liu, Y. Ren; Traveling pulse solutions of a generalized Keller-Segel system with small cell diffusion via a geometric approach, *J. Differential Equations*, **270** (2021) 1019-1042.

[7] N. Fenichel; Geometric singular perturbation theory for ordinary differential equations, *J. Differential Equations*, **31** (1979) 53-98.

[8] Q. Guo, H. Cheng; Existence of forced waves and their asymptotics for Leslie-Gower prey-predator model with some shifting environments, *Discrete Contin. Dyn. Syst. Ser. B*, **29** (2024) 2419-2434.
[9] Y. Hua, Z. Du, J. Liu; Dynamics of the epidemiological Predator-Prey system in advective environments, *J. Math. Biol.*, **89** (2024) 28-59.
[10] Y. Hua, X. Lin, J. Liu, et al; Dynamics of traveling waves for predator-prey systems with Allee effect and time delay, *Electron. J. Differential Equations*, **2024** No. 33 (2024) 1-19.
[11] J. Huang, M. Lu, C. Xiang, et al; Bifurcations of codimension 4 in a Leslie-type predator-prey model with Allee effects, *J. Differential Equations*, **414** (2025) 201-241.
[12] C. K. R. T. Jones; Geometric singular perturbation theory, Springer, Berlin, 1995.
[13] P. Kareiva, G. Odell; Swarms of Predators Exhibit "Preytaxis" if Individual Predators Use Area-Restricted Search, *Am. Nat.*, **130** (1987) 233-270.
[14] C. Kuehn; Multiple time scale dynamics, *Appl. Math. Sci.*, Springer, Switzerland **191** (2015).
[15] P. Leslie; Some further notes on the use of matrices in population mathematics, *Biometrika*, **35** (1948) 213-245.
[16] P. Leslie, J. Gower; The properties of a stochastic model for the predator-prey type of interaction between two species, *Biometrika*, **47** (1960) 219-234.
[17] D. Li; Global stability in a multi-dimensional predator-prey system with prey-taxis, *Discrete Contin. Dyn. Syst.*, **41** (2021) 1681-1705.
[18] D. Li, N. Tan, H. Qiu; Traveling wave solutions in a modified Leslie-Gower model with diffusion and chemotaxis, *Z. Angew. Math. Phys.*, **75** (2024) 165-188.
[19] J. Liu, J. Wu, X. Lin, et al; Traveling wave solutions of a diffusive predator-prey system with Holling II type functional response, *Proc. Amer. Math. Soc.*, **153** (2025) 577-589.
[20] A. Lotka; Elements of Physical Biology, Williams and Wilkins Company, Philadelphia, 1925.
[21] Q. Qiao; Traveling waves and their spectral instability in volume-filling chemotaxis model, J. Differential Equations, 382 (2024) 77-96.
[22] Q. Qiao, X. Zhang; Traveling waves to a chemotaxis-growth model with Allee effect, *J. Differential Equations*, **416** (2024) 1747-1770.
[23] H. Qiu, S. Guo; Steady-states of a Leslie-Gower model with diffusion and advectio, *Appl. Math. Comput.*, **346** (2019) 695-709.
[24] H. Qiu, S. Guo; Bifurcation structures of a Leslie-Gower model with diffusion and advection, *Appl. Math. Lett.*, **135** (2023) 108391.
[25] J. Roy, S. Dey, B. Kooi, et al.; Prey group defense and hunting cooperation among generalist-predators induce complex dynamics: a mathematical study, *J. Math. Biol.*, **89** (2024) 22-64.
[26] H. Safuan, I. Towers, Z. Jovanoski, et al.; On travelling wave solutions of the diffusive Leslie-Gower model, *Appl. Math. Comput.*, **274** (2016) 362-371.
[27] Z. Tian, L. Zhang; Traveling Wave Solutions for a Continuous and Discrete Diffusive Modified Leslie-Gower Predator-Prey Model, *Qual. Theory Dyn. Syst.*, **23** (2024) 253-301.
[28] V. Volterra; Fluctuations in the Abundance of a Species considered Mathematically, *Nature*, **47** (1926) 558-560.
[29] K. Wang, Z. Du, J. Liu; Traveling pulses of coupled FitzHugh-Nagumo equations with doubly-diffusive effect, *J. Differential Equations*, **374** (2023) 316-338.
[30] Y. Yao, J. He; Bifurcations of codimension three in a Leslie-Gower type predator-prey system with herd behavior and predator harvesting, *J. Appl. Anal. Comput.*, **15** (2025) 734-761.
[31] Z. Zhao, H. Hu; Boundedness, stability and pattern formation for a predator-prey model with Sigmoid functional response and prey-taxis, *Electron. J. Differential Equations*, **37** (2023) 1-20.
[32] H. Zhang, Y. Xia; Persistence of kink and anti-kink wave solutions for the perturbed double sine-Gordon equation, *Appl. Math. Lett.*, **141** (2023) 108616.
[33] W. Zhou, X. Wei; Global stability in a diffusive predator-prey model of Leslie-Gower type, *Partial Differ. Equ. Appl. Math.*, **7** (2023) 100472.

Shuna Wang
School of Mathematics and Statistics, Jiangsu Normal University, Xuzhou, Jiangsu 221116, China
*Email address*: 2020211141@jsnu.edu.cn

Jiang Liu
School of Mathematics and Statistics, Jiangsu Normal University, Xuzhou, Jiangsu 221116, China
*Email address*: jiangliu@jsnu.edu.cn

Jun Fang
School of Mathematics and Statistics, Jiangsu Normal University, Xuzhou, Jiangsu 221116, China
*Email address*: 2020231222@jsnu.edu.cn

Xiaojie Lin (corresponding author)
School of Mathematics and Statistics, Jiangsu Normal University, Xuzhou, Jiangsu 221116, China
*Email address*: linxiaojie@jsnu.edu.cn